JMEPEG (2020) 29:3411–3419
https://doi.org/10.1007/s11665-020-04810-0


1059-9495/$19.00

# Effect of Cold Rolling and Aging on the Microstructure and Mechanical Properties of Ti-Nb-Zr Alloy

*Feng He, Shuangping Yang, and Jimin Cao*

*(Submitted August 7, 2019; in revised form April 5, 2020; published online April 27, 2020)*

**The effect of cold rolling deformation and aging treatment on the phase transformation, microstructure evolution, and mechanical properties of a new Ti-Nb-Zr metastable β-titanium alloy was investigated by x-ray diffraction, scanning electron microscopy, transmission electron microscopy, and mechanical property testing. The results show that the alloy exhibited excellent phase stability that no stress-induced α″ phase transition occurred during cold rolling and that the plastic deformation mechanism was related to dislocation slipping. Interestingly, even under the same aging treatment at 300 °C for 2 h, the aging products for the unrolled and cold-rolled alloys are β + ω and β + α, respectively. The alloy with cold deformation produces a large number of dislocation defects, and grain boundaries inhibit the nucleation of the ω phase, while the α phase tends to nucleate at the dislocations and grain boundaries and promote the precipitation of the α phase. Compared with solution treatment and aging, the aging treatment after cold deformation has high-strength matching and its ideal elastic modulus can satisfy the requirements for dental implants.**

**Keywords** aging treatment, cold rolling, microstructure and mechanical property, Ti-Nb-Zr alloy

## 1. Introduction

Ti-25Nb-25Zr is a novel β-Ti alloy with good processing properties, high strength, and a low elastic modulus ( ≤ 80 GPa) because of the β-stabilizing element Nb and neutral element Zr. It shows excellent biocompatibility without toxic elements such as Al and V (Ref 1-3). It has broad market application prospects, especially for use in orthodontic stents, medical surgical implants, and hyperelastic spectacle frames.

Thermomechanical treatment is effective for improving strength and plasticity of Ti alloys (Ref 4). Compared with conventional heat treatments, it can increase the strength of Ti alloys by 20-40 kg/mm$^2$ without reducing the plasticity, as well as increase the strength by 5-10 kg/mm$^2$ and the plasticity by 1-1.5 times at the same time (Ref 5). Low-temperature deformation heat treatment processes start with a solid solution in the β phase region; an aging treatment is applied directly after cold deformation (Ref 6, 7). The dislocation defects from cold working accelerate the transformation of the secondary phase during heat treatment and hinder the movements of dislocations necessary for the transition of the β to the ω phase and favor the precipitation of the α phase (Ref 8, 9). At present, research on the aging treatment of near-β Ti alloys is focused on the precipitation of the ω and α phases as a result of the aging temperature and time. For example, studies by Gui-qin Shen and others on the decomposition characteristics of the β phase in Ti-15Mo-2.7Nb-3Al-0.2Si alloys during aging indicate that the secondary α phase is directly precipitated at temperatures greater than 500 °C but that the ω transition phase is precipitated at temperatures below 500 °C and gradually transforms into the α phase (Ref 10). For most near-β Ti alloys, the phase transition of β → ω → α occurs at a low aging temperature in the range from 250 to 500 °C (Ref 11, 12). The ω phase is ellipsoidal with high hardness and brittleness, which can substantially increase the strength, hardness, and elastic modulus of the alloy and drastically reduce the plasticity. When the volume fraction of the ω phase exceeds 80%, the alloy has no macroscopic plasticity; thus, the formation of the ω phase should be avoided (Ref 13). The ω phase is decomposed by raising the aging temperature and prolonging the aging time; however, such conditions tend to coarsen the α phase, which does not improve the mechanical properties (Ref 14). The size, shape, and volume fraction of the ω and α precipitates determine the degree of strengthening of the alloy (Ref 15, 16); however, little research has been reported on the strengthening mechanism from cold deformation during a low-temperature aging process. Exploring low-temperature deformation heat treatment processes for the new Ti-Nb-Zr alloy is important.

β-Ti alloys undergo a complicated phase transformation during aging, and the microstructure and properties are sensitive to thermomechanical treatment (Ref 17). No detailed information about the relationship among the microstructure evolution, phase stability, and mechanical properties is available. In this study, Ti-25Nb-25Zr alloy samples with different deformations were prepared by cold rolling, and the cold deformation characteristics of the alloy were studied. The temperature at which ω phase precipitation occurs (300 °C) was selected for aging with different cold deformation processes, and the relationships among the microstructure, morphology, phase transition behavior, and mechanical properties of the cold rolling and aging processes were revealed. We hope to modify the microstructure and properties by controlling the deformation and heat treatment, further elucidating the processing–structure–property correlation for the Ti-25Nb-25Zr

**Feng He** and **Shuangping Yang**, School of Metallurgical Engineering, Xi'an University of Architecture and Technology, Xi'an 710055, PR China; and **Jimin Cao**, Institute of Xi'an Seatell Metal Materials Co.Ltd, Xi'an 710018, PR China. Contact e-mail: hefeng1212@126.com.

alloy, which has the potential to be developed as an alloy for biomedical implants.

## 2. Experimental

To ensure chemical homogeneity, the Ti-Nb-Zr ingot was melted three times by vacuum consumable arc remelting with high-purity sponge titanium, sponge zirconium, and niobium chips. The transformation temperature $T_\beta = (650 \pm 10)$ °C was measured by differential scanning calorimetry (DSC). The ingot was forged at 1000 °C and then rolled to form a 10-mm bar at 850 °C in the β phase region. The bar was ground without defects, and then the solution was treated at 800 °C for 1 h and cooled in air. Bars with dimensions of $\phi$6.8 mm, $\phi$ 5.7 mm, and $\phi$4.7 mm were obtained by cold rolling with reductions of 24%, 47%, and 64%, respectively. The bars after solution treatment and cold rolling were aged at 300 °C to 600 °C for 0.5 h to 8 h.

The grain size and morphology of the samples after cold rolling deformation were observed by optical microscopy (OM) and scanning electron microscopy (SEM). The etching solution was composed of hydrofluoric acid, nitric acid, and water at a ratio of 1:3:7 (volume ratio). The phase composition and residual stress of the samples were determined via x-ray diffraction (XRD) analysis conducted on a Philips PW1700 x-ray diffractometer. The microstructure and dislocation morphology were observed by transmission electron microscopy (TEM) on a Talos F200X instrument; the samples for TEM observation were prepared by mechanical and ion reduction. The hardness was tested with a load of 10 kg and a loading time of 15 s, and five points for each sample were tested using an HV-10Z Vickers hardness tester. The mechanical properties of the alloy were evaluated by tension tests at room temperature.

## 3. Results and Discussion

### 3.1 Microstructure Characteristics of the Cold-Rolled Alloy

Figure 1 shows the XRD patterns of the Ti-Nb-Zr alloy before and after cold rolling. The microstructure of the alloy comprises a single β phase after cold rolling, similar to solution specimens, and the stress-induced α″ phase does not appear after cold rolling. In general, the cold deformation mechanism of β-Ti alloys is strongly dependent on the stability of the β phase at ambient temperature, where dislocation slip, twinning, and stress-induced martensitic transformation can occur during cold deformation (Ref 18, 19). The stability of the β phase during the cold deformation of β-Ti alloys determines whether stress-induced α″ martensite appears; the generation of the stress-induced α″ phase is unfavorable if the stability of the β phase is high. The *Ms* temperature of Ti-Nb-Zr alloys has been confirmed to decrease below room temperature when large amounts of Nb and Zr are present, and α″ martensite does not transform from the β phase. According to the principle of the *d*-electron orbital, two parameters (*Md* and *Bo*) are used to characterize and control the phase stability and properties of titanium alloys; if the *Bo* value is high and the *Md* value is low, the alloy is dominated by slip deformation with a very stable β phase (Ref 20-22). Therefore, for a Ti-5Al-5Mo-5 V-3Cr-1Zr alloy with *Bo* = 2.29 and *Md* = 2.771, the β phase is highly stable and no stress-induced α″ phase appears during cold deformation (Ref 23). These parameters obviously affect the mechanism of cold deformation. According to calculations, the Ti-Nb-Zr alloy with *Bo* = 2.896 and *Md* = 2.528 has high β stability. The stress-induced α″ phase does not form during the cold deformation process, which is consistent with the XRD test results shown in Fig. 1. As the amount of cold rolling deformation increases, the alloy generates an increasing amount of internal stress and small grains, resulting in a broadening of the diffraction peaks.

The initial morphology after the solid solution treatment at 800 °C for 1 h comprises a single equiaxed β phase with an average grain size of 67 μm, as shown in Fig. 2. The microstructure of the alloy gradually changes with increasing cold rolling deformation. After the cold rolling deformation reaches 47%, equiaxed β grains with a size of 32 μm are crushed and elongated in the rolling direction and deformation bands are observed within the deformed grains (Fig. 3b and e). After 64% cold deformation, the grain size becomes 14 μm and β grain boundaries are broken with apparent more fibrous shear bands in the rolling direction, as can be illustrated by OM in Fig. 3(c) and (f). The average hardness of solid solution alloy was 195 Hv, and the deformed microstructure increased

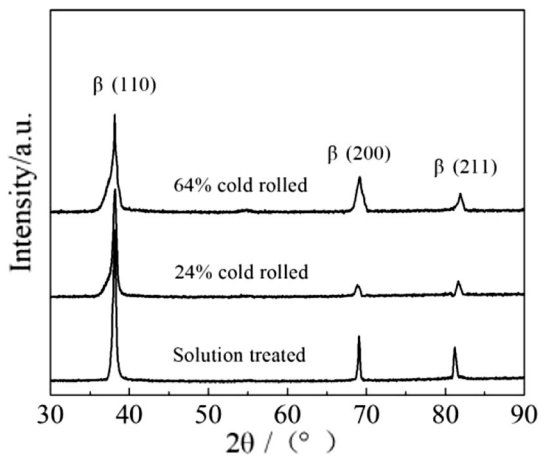


**Fig. 1** XRD patterns of alloy cold-rolled to 24 and 64% reductions

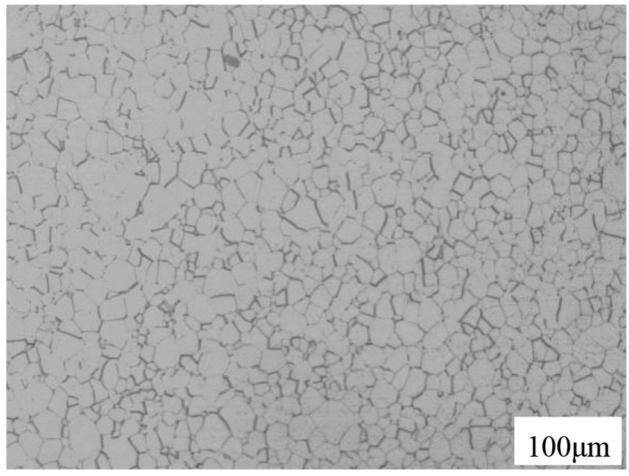


**Fig. 2** OM images of alloy after solution treatment

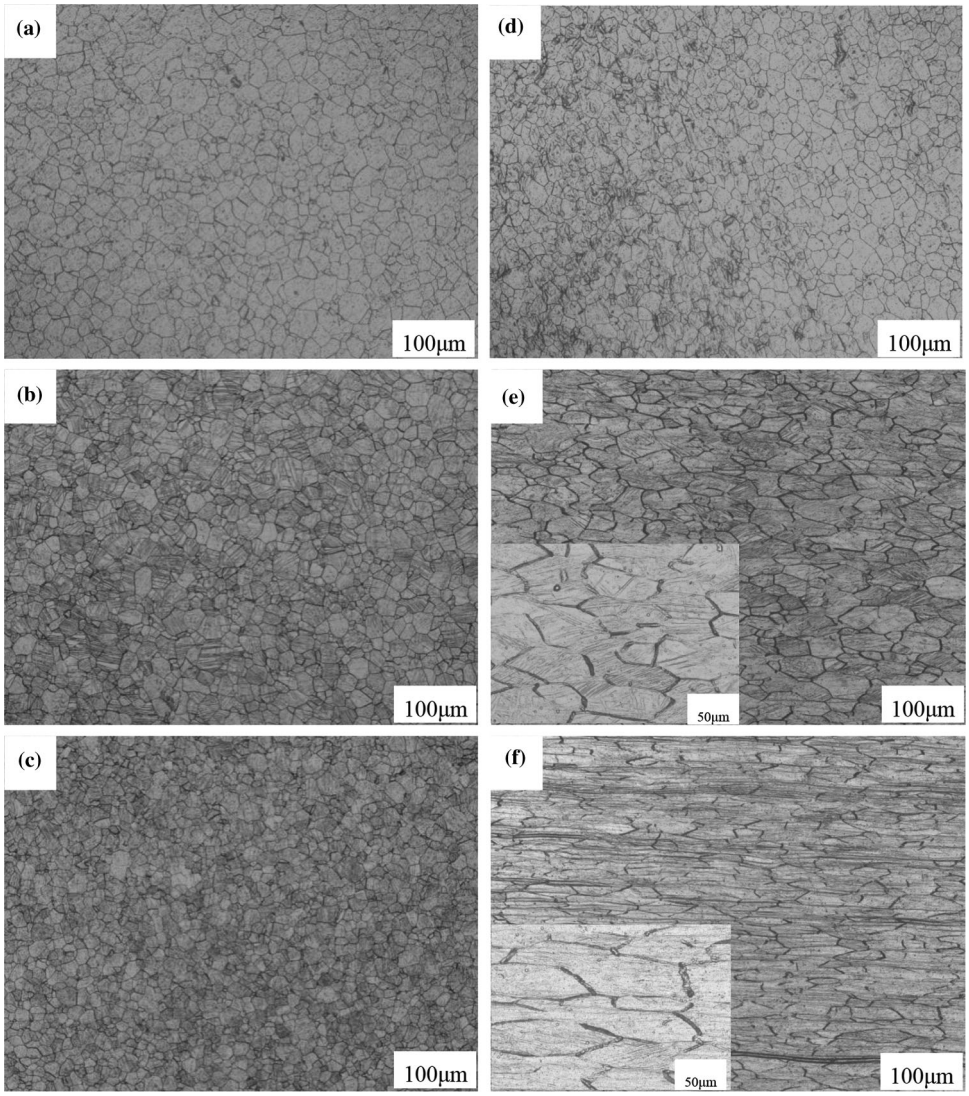


**Fig. 3** OM images of alloy after cold deformation: (a), (d) ε = 24%; (b), (e) ε = 47%; (c), (f) ε = 64%; (a), (b), (c) transverse; (d), (e), (f) longitudinal

hardness values to 286 Hv after 64% cold deformation. In addition, the results related to the alloy with high β stability show that no strain-induced phase transformation occurs and that the cold rolling induces substantial strengthening due to strain hardening with an abundance of dislocation defects.

### 3.2 Effect of Aging Treatment After Cold Deformation on the Phase Transformation and Microstructure

Figure 4 shows the microstructure of different cold rolling deformations after treatment at 300 °C for 2 h. The sample without deformation shows no α phase precipitates at this temperature, and the small and white ellipsoidal ω phase is observed in the β matrix under SEM (Fig. 4a) to have high dispersion. A dark-field micrograph and selected-area diffraction (SAD) pattern of the unrolled alloy are presented in Fig. 5(a) and (c), where the diffraction spots are viewed along the $[113]_\beta$ zone axis and are associated with the ω phase. The ellipsoidal ω phase precipitates are characteristic of the isothermally formed precipitates in low-misfit alloy systems (Ref 24). The ω phase is a supersaturated solid solution of a β-stabilizing element in α-Ti. During decomposition of the β phase, the $\beta \rightarrow \omega + \beta$ aging transition occurs very quickly, where the co-precipitates have a small particle size and high particle density. The alloy without cold rolling has low dislocation and grain boundary densities, and shearing easily occurs, resulting in a large number of aging ω phase precipitates (Ref 14).

In contrast to the microstructure during cold deformation, the ω phase disappears and a large amount of acicular α phase precipitates under the same aging treatment as shown in Fig. 4(b). Interestingly, lath precipitated in the β matrix, as indicated by the white arrow in Fig. 5(b). The SAD pattern in Fig. 5(d) also shows that the precipitates were α phase. As cold rolling deformation increases, small and dense α phase precipitates appear on the surface. When the cold deformation reaches 64%, the entire substrate surface is covered by a dense α phase, as shown in Fig. 4(d). Thus, the cold deformation can promote the precipitation of the α phase, mainly because the ω phase nucleates from the β phase through coherent shear without diffusion, whereas the cold rolling produces a large number of dislocation defects and grain boundaries inhibit the nucleation of the ω phase. However, α phase easily nucleates at

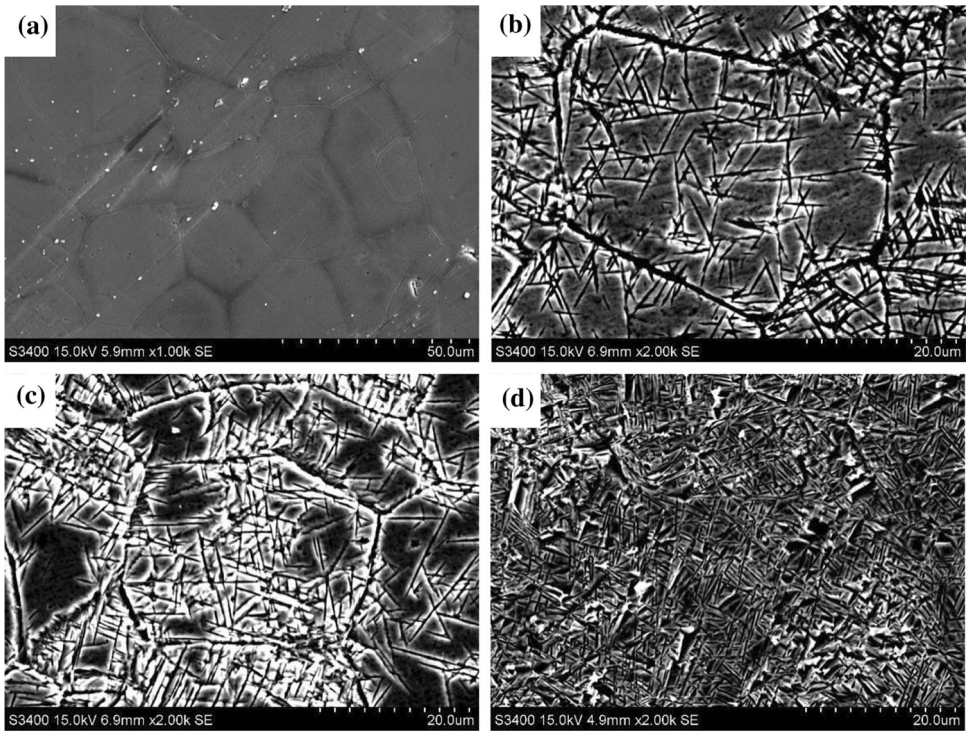


**Fig. 4** SEM micrographs of specimen after cold rolling followed by aging at 300 °C for 2 h; (a) unrolled, (b) 24% cold-rolled, (c) 47% cold-rolled, (d) 64% cold-rolled

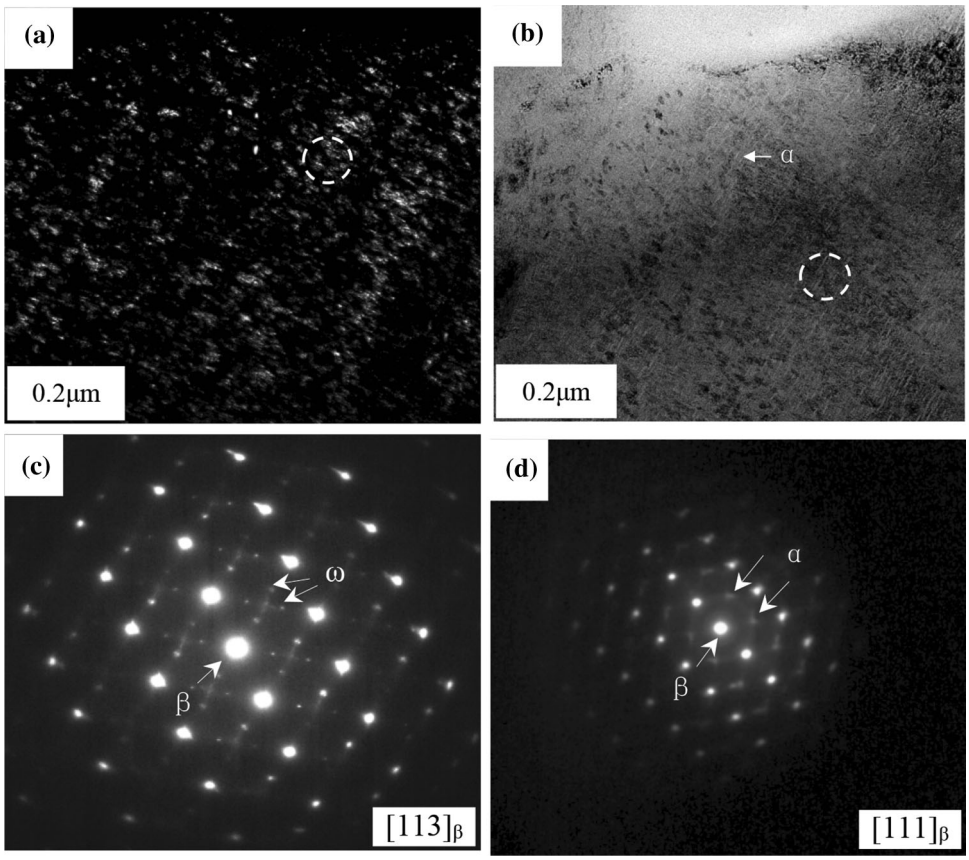


**Fig. 5** TEM images of Ti-Nb-Zr alloy aged at 300 °C for 2 h: the unrolled alloy (a) dark field, (c) SAD pattern; the 26% cold rolling alloy (b) bright field, (d) SAD pattern

dislocations and grain boundaries, which promote the precipitation of α phase. Furthermore, the alloy without cold deformation has an insufficient phase-change driving force to undergo the phase transformation of β → ω → α; however, the cold deformation produces numerous dislocation defects that increase the free energy of the alloy and the phase-change driving force, which promotes the direct precipitation of the α phase from the β matrix. Therefore, cold rolling of the Ti-Nb-Zr alloy produces a large number of dislocations and grain boundaries that can hinder the precipitation of the ω phase and promote the precipitation of a dispersed α phase during the subsequent low-temperature aging treatment, which results in a good combination of high strength and low modulus.

### 3.3 The Effect of Cold Rolling and Aging on Mechanical Properties

Figure 6 shows the representative stress–strain curves of alloy with solution treatment, cold rolling and cold rolling followed by aging. It can be noticed that the solution specimen did not present typical double yielding feature because the Ti-Nb-Zr alloy exhibited excellent phase stability. Furthermore, the ductility of alloy was higher and the strength was lower with increasing aging temperatures. The alloy with 64% cold deformation aged at 350 °C had higher strength than other specimens, and the specimen did not show plastic stage during the tension testing. The tensile properties of alloy were mainly affected by the size of precipitation phase and grain boundaries, which would inhibit the slip of alloy during tension testing.

Figure 7 shows the hardness, tensile strength, elongation, and elastic modulus of the Ti-Nb-Zr alloy aged at different temperatures with cold rolling deformations. Hardness is the ability of a material to resist elastic deformation, plastic deformation, and damage. The average hardness and tensile strength first increased and then quickly decreased; the ductility changes in an opposite manner with increasing aging temperature. Meanwhile, the unrolled alloy reached the peak value of 396 Hv and 1028 MPa, but the lowest elongation at 400 °C, which was different from the values for cold-rolled alloys. At the same aging temperature, the hardening effect of the alloy becomes more significant because the amount of cold deformation increases and the hardness of the alloy that experienced 64% cold deformation reached a peak value of 430 Hv and 1250 MPa; the elongation reached the lowest value of 6% at 350 °C. It had poor ductility and showed a macro-fracture that

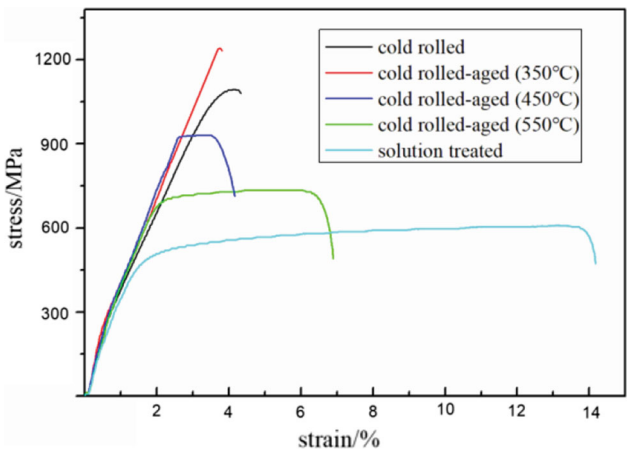


**Fig. 6** Tensile stress–strain curves of alloy under different treated

was very flat as shown in Fig. 8(a), which is a characteristic of brittle fracture.

However, after subsequent aging at higher temperatures, the alloy exhibits the greatest elongation and lowest average hardness and tensile strength, which were almost similar to those of solution samples. Figure 8(b) shows that many more cleavage planes and small shallow dimples appeared on the fracture surface of the sample aged at 400 °C; furthermore, the fracture morphologies exhibited ductile fracture in the samples for which the macro-fracture was fibrous and the micro-fracture had many more dimples and holes at 500 °C in Fig. 8(c), which was typical of ductile fracture and had high plasticity. According to the aforementioned analysis of the unrolled alloy, only a large amount of ω phase precipitated at low temperatures. The ω phase is the hard phase; it improves the hardness and strength of the alloy, but drastically decreases its ductility. As the amount of cold deformation increases, cold working produces more dislocation defects and grain boundaries inside the alloy and provides numerous sites for nucleation; the needlelike α phase can precipitate quickly and substantially at low temperatures, which increases the hardness and tensile strength of the alloy by dislocation strengthening and precipitation strengthening. When the aging temperature is greater than 350 °C, the hardness decreases as the aging temperature increases, not only because the strengthening effect is weakened due to growth and coarsening of the α phase but also because the residual stress and dislocations due to cold working are recovered at a high temperature. Figure 9(c) and (e) shows that a small net-shaped phase was interlaced inside grains at 500 °C and exhibited a recrystallized structure with only equiaxed β phase at 600 °C. The coexistence of these two effects leads to the alloy being softened instead of hardened.

The elastic modulus of alloys dominantly influences the e/a ratio and the precipitation phase. From Fig. 7(d), the elastic modulus was decreased with increasing aging temperature, the unrolled alloy reached the peak value to 87 GPa at 400 °C, and the 64% cold deformation alloy reached the peak value of 82 GPa at 300 °C. These results are attributed to the β → β + ω → β + ω+α → β + α phase transformation occurring during the aging treatment, where the ω phase and α phase increase the elastic modulus of β-Ti, and the effect of increase in the elastic modulus is in the following order: ω > α > β. With increasing aging temperature, the α phase continuously precipitates and the ω phase decomposes, leading to a lower elastic modulus. The cold rolling promoted the precipitation of α phase at low temperatures to decrease the elastic modulus. Therefore, the combination of phase transformation and dislocation strengthening would achieve an alloy with high-strength plasticity matching and an ideal elastic modulus.

By evaluating the results for the same aging temperature but different aging times, we found that the hardness and tensile strength first increased and then decreased, whereas the ductility changed in an opposite manner over time. In addition, the alloy reached a peak value in a short time with a large amount of cold deformation, as shown in Fig. 10. The transformation of β → ω → α occurred during the aging process of the Ti-Nb-Zr alloys and required sufficient time for the conversion process. When the unrolled alloy was aged at 300 °C for a short time, the ω phase precipitated and contributed to precipitation strengthening. Over time, the volume fraction of the precipitated ω phase increased gradually and the hardness, tensile strength, and the elastic modulus increased; however, the elongation decreased rapidly. We

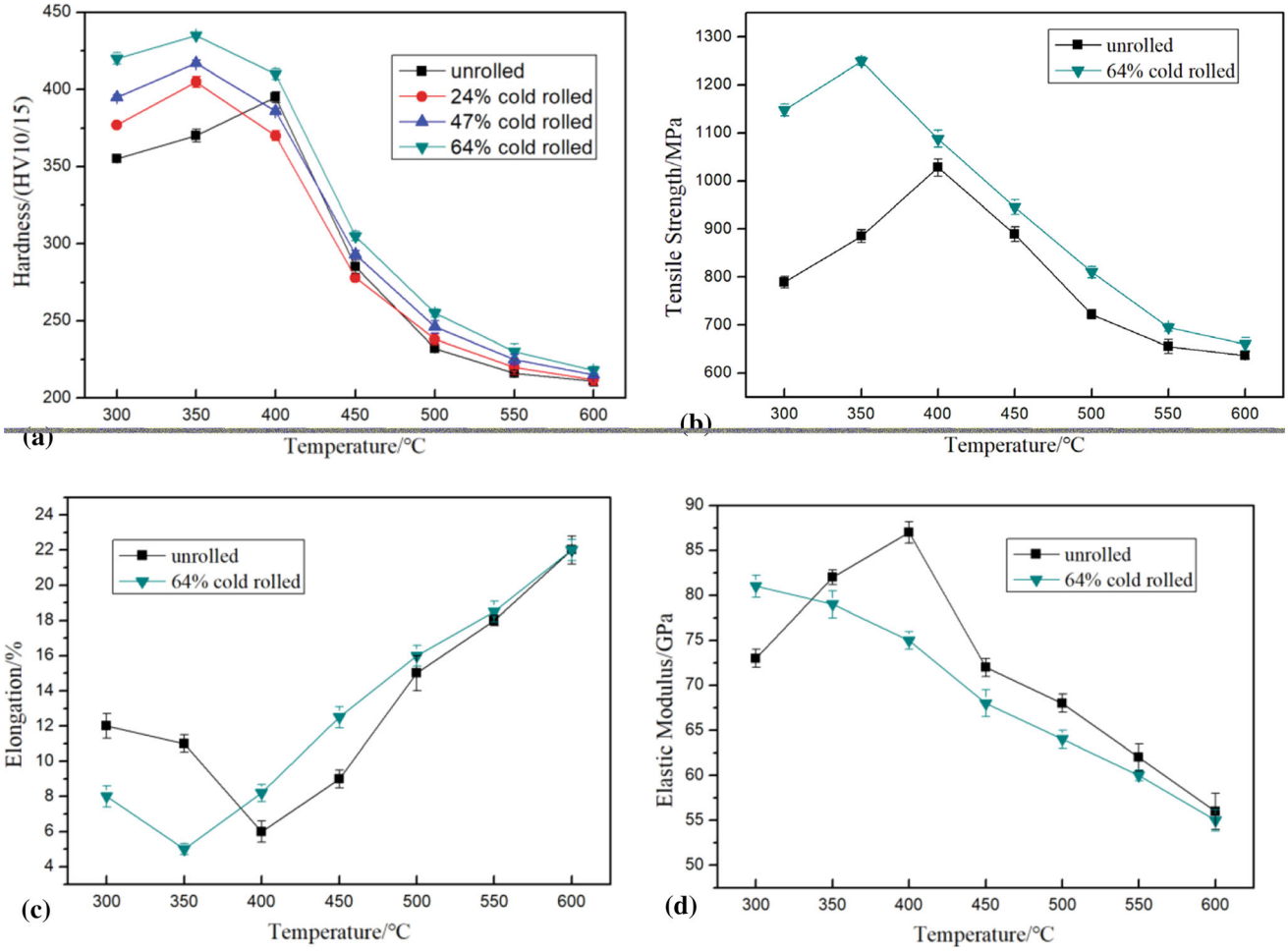


**Fig. 7** Mechanical properties of alloy by cold rolling followed by aging at 300-600 °C for 2 h

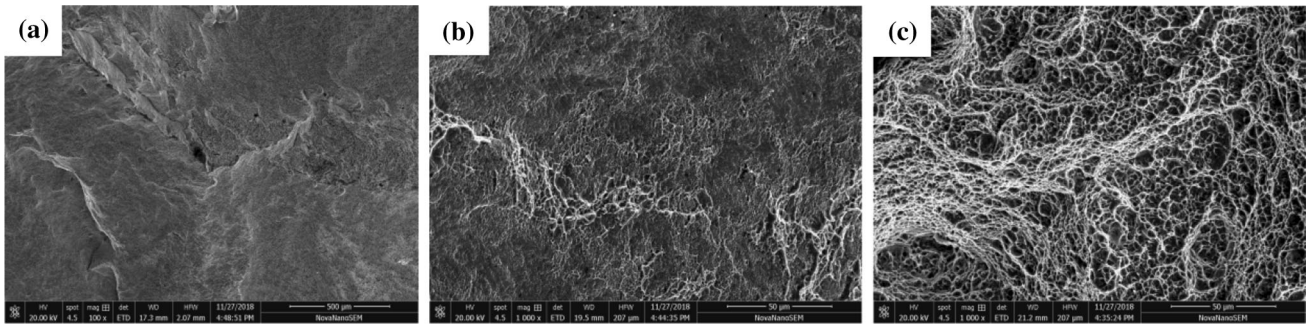


**Fig. 8** SEM fractographs of sample with different aging temperatures (a) 350 °C, (b) 400 °C, (c) 500 °C

observed that the aging time was beneficial with respect to the amount of phase precipitation. When the aging time was extended to 6 h, the hardness, tensile strength, and elastic modulus of the unrolled alloy reached peak values of 415 Hv, 1180 MPa, and 92 GPa, respectively. Thus, the peak value decreased slightly with increasing volume fraction of the ω phase and decreased with increasing precipitation of the α phase because the precipitates of the ω phase exhibited a much higher strengthening effect and elastic modulus than the α phase precipitates.

The phase transformation speed of an alloy is mainly determined by its phase-change driving force and the diffusion rate of the solute atoms (Ref 25). The alloy without cold deformation exhibits an insufficient phase-change driving force to actuate the phase transformation of β to α. However, cold working and generating a large amount of nonequilibrium defects can increase the free energy of the alloy, which can increase the phase-change driving force, promote the precipitation of the α phase, and shorten the aging time at low temperatures. The α phase with high strength and low elastic modulus impart the alloy with excellent integrated performance. However, the long aging time led to overaging and decreased the hardness and tensile strength of the alloy because the α phase began to agglomerate and grow. As shown in

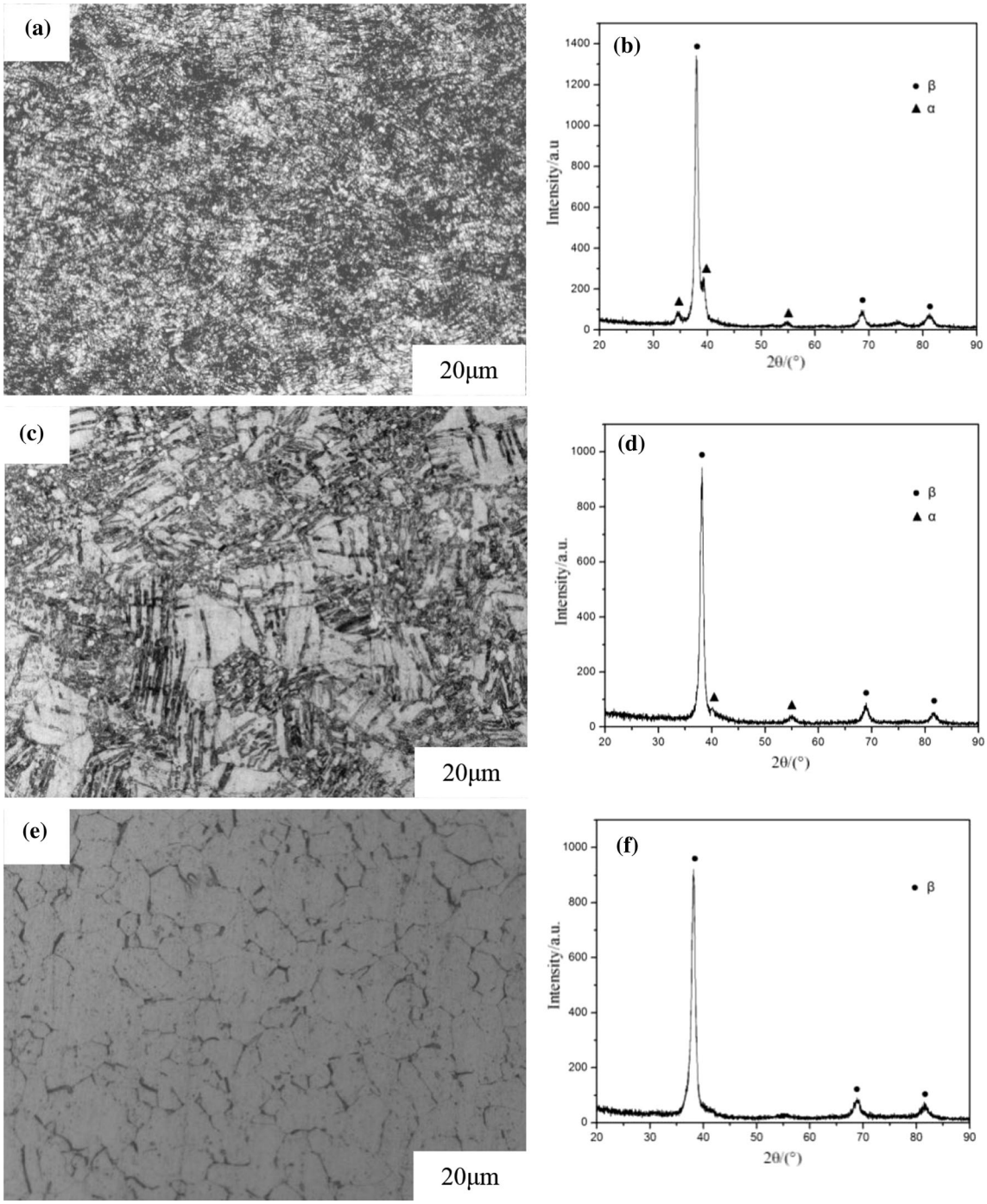


**Fig. 9** OM images and XRD profiles of specimen with different aging temperatures: (a), (b) 400 °C, 2 h, (c), (d) 500 °C, 2 h, (e), (f) 600 °C, 2 h

Fig. 10, with increasing aging time, the hardness, and tensile strength peak value with 64% cold rolling deformation was shortened from 6 to 3 h compared with that without cold rolling. When the aging time was 3 h, the cold-rolled sample had more α phase precipitation than unrolling alloy (Fig. 11). The shorter aging time is not conducive to the growth of the α phase, which is a great advantage for improving the strength of the alloy.

## 4. Conclusion

The phase transformation and microstructure evolution of a Ti-Nb-Zr alloy were studied as a function of cold deformation and aging. The experimental results showed that the alloy had high β stability, with dislocation slip occurring during cold rolling and no stress-induced martensitic α″ phase transformation from the β matrix. The alloy with cold deformation

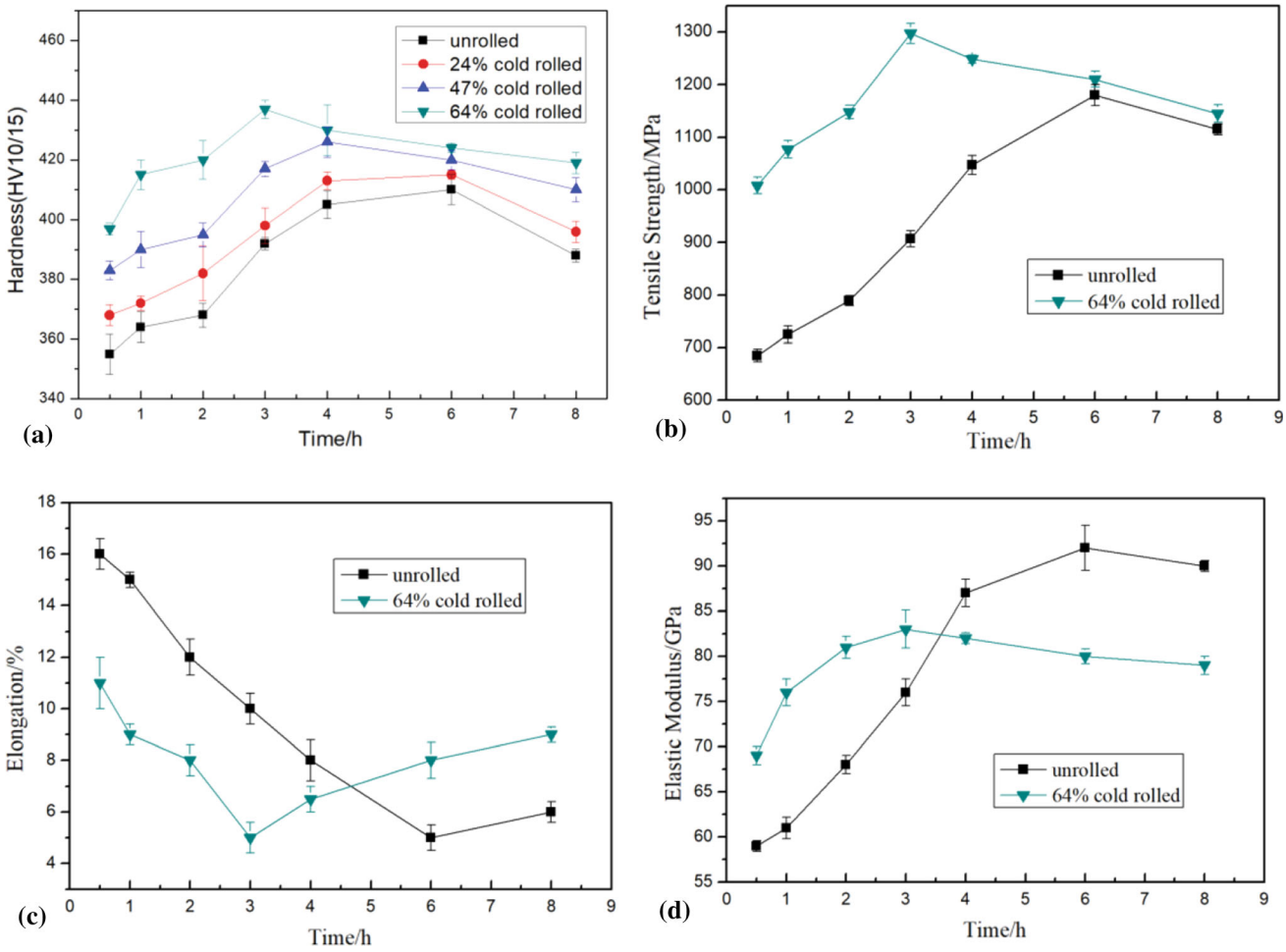


**Fig. 10** Mechanical properties of alloy by cold rolling followed by aging at 300 °C for 0.5-8 h

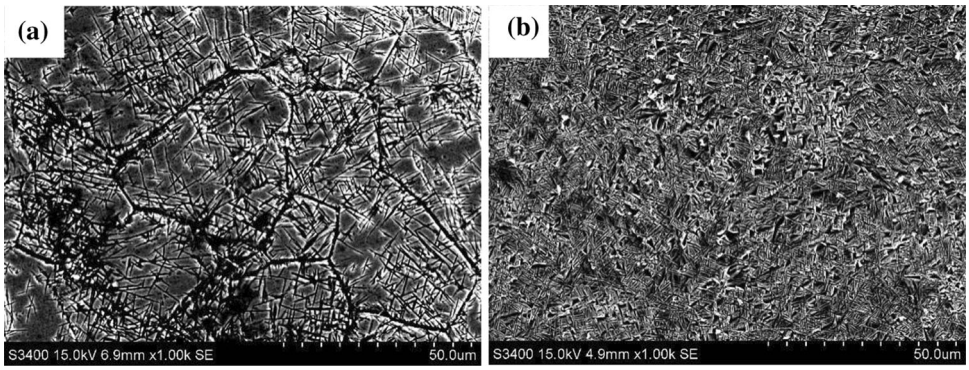


**Fig. 11** SEM images of alloy aged at 300 °C for 3 h; (a) unrolled, (b) 64% cold-rolled

produced a large number of dislocation defects, and grain boundaries inhibited the nucleation of the ω phase, whereas the α phase tended to nucleate at the dislocations and grain boundaries, which promoted the precipitation of the α phase. After the solution and cold-rolled alloys were aged at 300 °C for 2 h, the phase compositions of the alloy were β + aging ω phase and β + α phase, respectively. With increasing aging temperature and time, the hardness and tensile strength of the alloy first increased and then decreased, and the peak value with increasing deformation appeared after treatment at 350 °C for 3 h. The aging strengthening of cold-rolled Ti-Nb-Zr alloy was composed of dispersion strengthening from the α phase and strain hardening. Compared with the solution and aging treatment, the aging treatment after cold deformation has high-strength matching and the resulting ideal elastic modulus can meet the requirement for dental implants.

## Acknowledgments

The authors would like to gratefully acknowledge that this work was supported by the National Natural Science Foundation of China under Grant No. 51604208.

## References

1. T.M. Mohsin, Development of a New Metastable Beta Titanium Alloy for Biomedical Applications, *Karbala Int. Modern Sci.*, 2017, **3**, p 225–227
2. X. Wang, L.G. Zhang et al., Study of Low-Modulus Biomedical β Ti-Nb-Zr Alloys Based on Single-Crystal Elastic Constants Modelling, *J. Mech. Behav. Biomed. Mater.*, 2016, **4**, p 310
3. N. Mitsuo, Mechanical Biocompatibilities of Titanium Alloys for Biomedical Applications, *J. Mech. Behav. Biomed. Mater.*, 2007, **1**, p 30–35
4. Y.L. Zhou and D.M. Luo, Microstructures and Mechanical Properties of Ti-Mo Alloys Cold-Rolled and Heat Treated, *Mater. Charact.*, 2011, **62**(10), p 931–934
5. X.L. Ning, Deformation Heat Treatment of Titanium Alloy, *Rare Metal Mater. Eng.*, 1982, **1**, p 59–61
6. Z.B. Zhao, Q.J. Wang et al., Effect of β (110) Texture Intensity on α-Variant Selection and Microstructure Morphology During β → α Phase Transformation in Near α Titanium Alloy, *Acta Mater.*, 2017, **126**, p 372–375
7. T.A. Sokolova, B.K. Sokolov, and I.V. Gervaseva, Hydrogen Effect on the Texture and Mechanism of Deformation Upon Cold Rolling of a Beta-Titanium Alloy, *Phys. Met. Metall.*, 1999, **88**(3), p 301–305
8. L.Q. Wang, W.J. Lu, J.N. Qin et al., Effect of Precipitation Phase on Microstructure and Superelasticity of Cold-Rolled Beta Titanium Alloy During Heat Treatment, *Mater. Des.*, 2009, **30**(9), p 3873–3878
9. S. Guo, Q.K. Meng, L. Hu et al., Suppression of Isothermal ω Phase by Dislocation Tangles and Grain Boundaries in Metastable β-type Titanium Alloys, *J. Alloy. Compd.*, 2013, **550**, p 35–38
10. G.Q. Shen, B. Xu, Y.Q. Peng et al., Phase Transformation in Ti-15Mo-2.7Nb-3Al-0.2Si High Strength Titanium Alloy, *Mater. Eng.*, 1999, **3**, p 19–25
11. C. Li, *Tailoring the Mechanical Properties of Titanium Alloys via Stress-Induced Martensitic Transformation*, Hunan University, Hunan, 2013, p 16–19
12. B. Sander and D. Raabe, Texture Inhomogeneity in a Ti-Nb-Based β-Titanium Alloy After Warm Rolling and Recrystallization, *Mater. Sci. Eng.*, 2008, **479**(1–2), p 236–240
13. S.K. Li, Y.W. Yu, Z.Q. Liao et al., Effect of ω Phase on Properties of Ti10V2Fe3Al Alloy, *Chin. J. Nonferrous Metals*, 2010, **20**, p 387–391
14. L. Hu, S. Guo et al., Effect of Thermo-Mechanical Treatment on Microstructure and Mechanical Property in Metastable β Titanium Alloy, *Rare Metal Mater. Eng.*, 2015, **44**(1), p 146–148
15. G.C. Obasi, D. Rugg et al., The Effect of β Grain Coarsening on Variant Selection and Texture Evolution in a Near-β Ti Alloy, *Mater. Sci. Eng. A*, 2013, **576**, p 272–275
16. H.Y. Kim, Y. Ikehara et al., Martensitic Transformation, Shape Memory Effect and Superelasticity of Ti-Nb Binary Alloys, *Acta Mater.*, 2006, **54**, p 2419–2423
17. Q. Guo, Q. Wang, X.L. Han et al., Precipitation Behavior of α Phase and Mechanical Properties in Severely Plastic Deformed Ti-15-3 Alloy, *Rare Metal Mater. Eng.*, 2011, **44**(3), p 0377–0379
18. L.Q. Wang, *Characteristics of Cold Deformed and Superelasticity of TiNbZrTa Beta Titanium Alloy*, Shanghai Jiaotong University, Shanghai, 2009, p 12–18
19. S. Sadeghpour, S.M. Abbasi, and M. Morakabati, Deformation-Induced Martensitic Transformation in a New Metastable β Titanium Alloy, *J. Alloy Compd.*, 2015, **650**, p 22–25
20. M. Morinaga, M. Kato, T. Kamiura et al., Theoretical Design of β-Type Titanium Alloys, *Sci. Technol.*, 1992, **1**, p 217–221
21. H. Matsumoto, S. Watanabe, and S. Hanada, Microstructures and Mechanical Properties of Metastable β TiNbSn Alloys Cold Rolled and Heat Treated, *J. Alloy. Compd.*, 2007, **439**, p 146–149
22. N. Nomura, T. Kohama et al., Mechanical Properties of Porous Ti-15Mo-5Zr-3Al Compacts Prepared by Powder Sintering, *Mater. Sci. Eng. C*, 2005, **25**, p 330–335
23. F.W. Chen, X.Y. Zhan, and K.C. Zhou, Effect of Cold Rolling on Microstructure Characteristics and Subsequent Aging Behavior and Mechanical Property of TRarei-55531 Alloy, *Metal Mater. Eng.*, 2015, **44**(7), p 1719–1722
24. D. Kent, S. Pas, and S.M. Zhu, Thermal Analysis of Precipitation Reactions in a Ti-25Nb-3Mo-3Zr-2Sn Alloy, *Appl. Phys. A*, 2012, **107**, p 835–841
25. C.B. Lan, Y. Wu, L.L. Guo et al., Microstructure, Texture Evolution and Mechanical Properties of Cold Rolled Ti-32.5Nb-6.8Zr-2.7Sn Biomedical Beta Titanium Alloy, *J. Mater. Sci. Technol.*, 2017, **34**, p 781–788